

**SUPPLEMENTAL MATERIAL FOR “PRESSURE-DEPENDENT SHEAR RESPONSE OF JAMMED PACKINGS OF FRICTIONLESS, SPHERICAL PARTICLES”**

This Supplemental Material presents additional results that support the conclusions in the main text. First, in Sec. A, we determine the small fraction of geometrical families with shear moduli that increase with pressure. In Sec. B, we examine the distribution of packing fractions at jamming onset  $P(\phi_J)$  collected over a range of shear strains. We also calculate the probability of compression unjamming (averaged over a range of shear strain and at fixed zero shear strain) and show that the probability remains nonzero in the large system-size limit. Finally, in Sec. C, we describe the algorithm that we use to detect rattler particles in overcompressed, frictionless disk and sphere packings.

**A. Shear moduli  $G^i$  of packings within geometrical families that increase with pressure**

The main text asserts that only a small fraction of the geometrical families for disk and sphere packings have shear moduli that linearly increase with pressure, rather than decrease. In Fig. 1, we plot the fraction of geometrical families  $N_{inc}/N_{tot}$  with shear moduli  $G^i$  that linearly increase with pressure, for four system sizes ( $N = 64, 128, 256,$  and  $512$ ) of disk packings, as well as  $N = 64$  sphere packings. We find that  $N_{inc}/N_{tot}$  is non-zero (but extremely small  $< 0.45\%$ ) in the large-pressure regime, yet the fraction decreases to zero in the large-system limit.

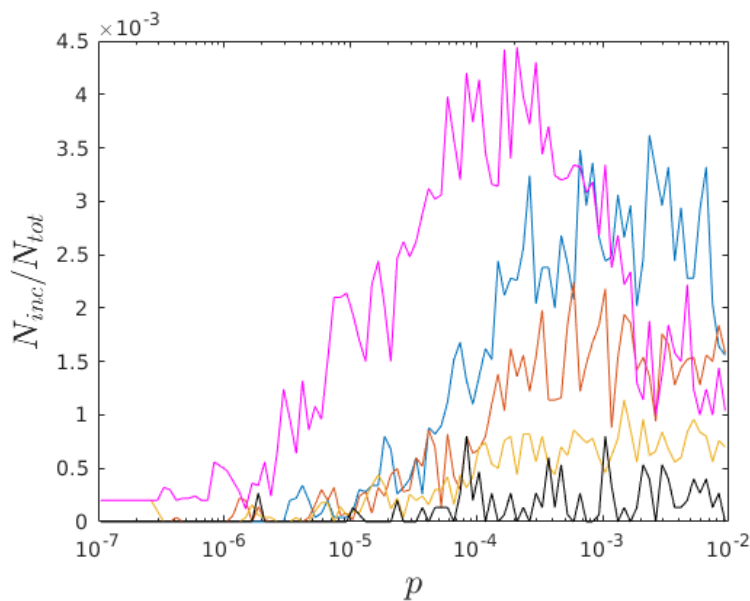


FIG. 1. We plot the fraction of configurations  $N_{inc}/N_{tot}$  that are within a geometrical family with a shear modulus  $G^i$  that linearly increases with  $p$  for jammed bidisperse disk packings with  $N = 64$  (blue),  $128$  (red),  $256$  (orange), and  $512$  (black), as well as bidisperse sphere packings with  $N = 64$  (pink). In all cases,  $N_{inc}/N_{tot} < 0.45\%$ . The anomalous geometrical families with shear moduli that increase with  $p$  are more prevalent in the high-pressure regime, but become increasingly infrequent as the system-size increases.

**B. Distribution of packing fractions at jamming onset  $\phi_J$**

To gain a better understanding of the nature of compression unjamming, we generated pressure contours as a function of  $\phi$  and  $\gamma$  for two additional system sizes for disk packings,  $N = 128$  and  $256$ , in Fig. 2. We find that the range of  $\phi$  over which compression unjamming occurs decreases with increasing system size, which is consistent with the fact that the distribution of jamming onsets  $P(\phi_J)$  narrows to a  $\delta$ -function at  $\phi_J^\infty \approx 0.842$  in the large-system limit for athermal packing-generation protocols.

In Fig. 3 (a), we plot the mean of the upper and lower  $\phi_J$  values over all shear strains where compression unjamming occurs, and we find that the difference between the two decreases with increasing system size. In addition, the standard

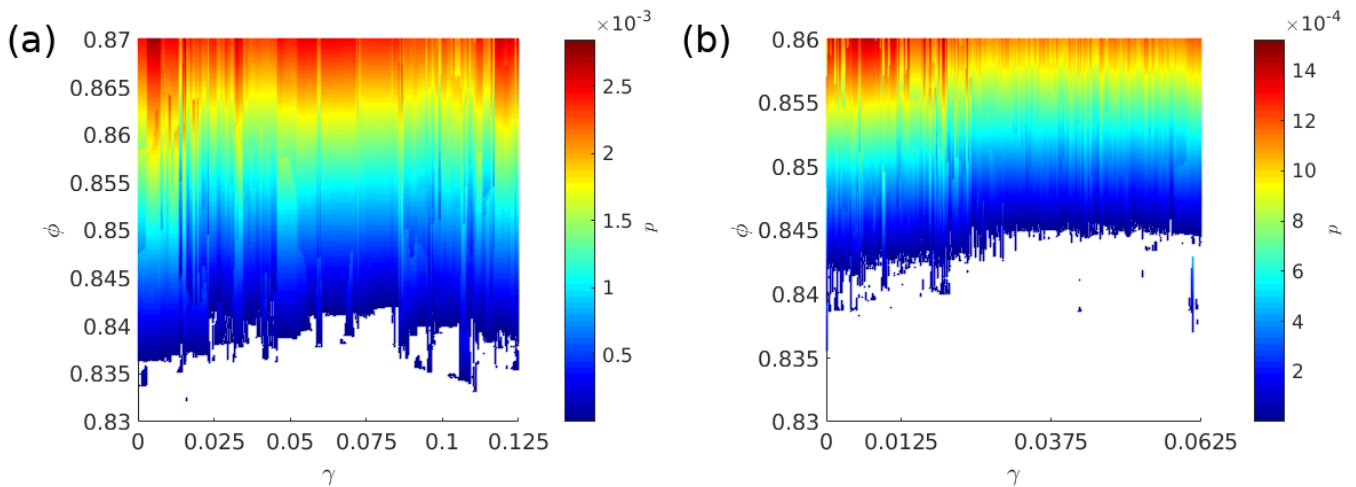


FIG. 2. Contour plots of the pressure  $p$  as a function of shear strain  $\gamma$  and packing fraction  $\phi$  originating from a single packing of bidisperse disks with  $\gamma = 0$  and the following system sizes and initial packing fractions: (a)  $N = 128$ ,  $\phi_i = 0.83$  and (b)  $N = 256$ ,  $\phi_i = 0.83$ . White regions correspond to unjammed packings with  $p = 0$ , and  $p$  increases from dark blue to maroon.

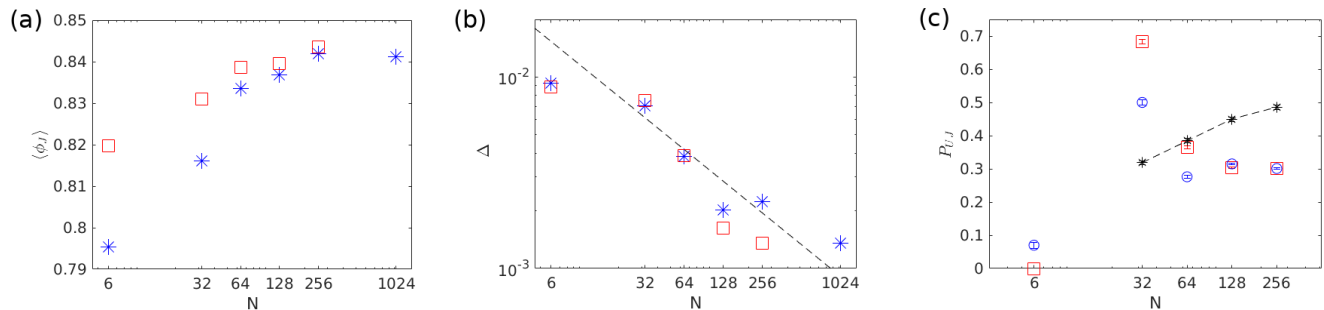


FIG. 3. (a) The average packing fraction at jamming onset  $\langle \phi_J \rangle$  versus system size  $N$  for bidisperse disks, averaged over every  $\gamma$  at which compression unjamming occurs. The blue asterisks represent the initial (lower)  $\phi_J$  values before compression unjamming occurs, and the red squares represent the final (higher)  $\phi_J$  values after compression re-jamming occurs. The  $N = 1024$  data was obtained from an ensemble of jammed packings at  $\gamma = 0$ . (b) The standard deviation  $\Delta$  for the packing fraction distributions whose means are plotted in (a). The black dashed line has slope  $-0.55$ . (c) The probability of compression unjamming  $P_{UJ}$  as a function of system size  $N$ , calculated as the number of shear strain values at which compression unjamming occurs divided by the total number of shear strain values sampled. The red squares give the probability over the same range of strain for all system sizes, and the blue circles give the probability over all sampled shear strains for each system. The black asterisks give the probability of compression unjamming for 5000 bidisperse disk packings compressed above jamming onset, and the dashed line shows a best fit to the function  $P_{UJ} = P_f - ae^{N/N^*}$ , where  $a = 0.492 \pm 0.019$  and  $N^* = 67.5 \pm 22.3$ .

deviation of the packing fraction at which compression unjamming occurs decreases with increasing system size as a power law with an exponent that is similar to the one ( $\Omega \sim 0.55$ ) that characterizes the narrowing of the distribution of packing fractions at jamming onset with increasing  $N$  for athermal packing-generation protocols. (See Fig. 3 (b).) However, even though the range of packing fractions over which compression unjamming occurs is decreasing with increasing system size, this does not imply that the probability of compression unjamming tends to zero in the large-system limit.

We find that the probability of compression unjamming  $P_{UJ}$  averaged over a fixed range of shear strain reaches a finite value  $P_{UJ} \sim 0.3$  in the large-system limit, as shown in Fig. 3 (c). We also generated ensembles of 5000 bidisperse disk packings at  $\gamma = 0$  for system sizes  $N = 32, 64, 128,$  and  $256$ , compressed to 1000 values of packing fraction, equally spaced from  $\phi_i = 0.8$  to  $\phi_f = 0.85$ . For each system size, we calculated the probability that the system changes from jammed to unjammed  $P_{UJ}$  during compression. The probability in the large-system limit approaches  $P_{UJ} \sim 0.5$ , which is larger than the compression unjamming probability obtained when the packings are sheared.

### C. Rattler-detection algorithm

For any disordered, overcompressed jammed packing of frictionless spherical particles in  $d$  spatial dimensions, it is possible to determine exactly the rattler particles that do not contribute to the packing's mechanical stability. A particle is a rattler in a jammed packing if and only if there does not exist a set of  $d + 1$  of its interparticle contact forces for which one can assign nonzero force magnitudes to attain a net zero force.  $d + 1$  contacts are required to constrain all of the  $d$  translational degrees of freedom of each particle [1–3]. (Note that this algorithm does not apply to non-spherical particles, which possess rotational degrees of freedom that require varying numbers of contacts to constrain them [4, 5].) We specify that the packing must be disordered to prevent degenerate sets of contacts from appearing in the packing which are collinear, coplanar, and so on. Hence, for every particle in the jammed packing, we identify whether or not it is a rattler by checking every subset of  $d + 1$  of its contacts, and determining whether or not it is possible to obtain zero net force.

This method is equivalent to checking whether or not all of the contacts are on one “side” of the particle. In other words, is it possible to split the particle into two  $d$ -dimensional hemispheres such that all of the contacts lie on only one of the hemispheres? In this case, the contact forces cannot be balanced because any set of non-zero force magnitudes will yield a net force that can push the particle in the direction of the other hemisphere. However, if it is impossible to do this, the contact forces can be balanced since any net force from  $d$  of the contacts can be balanced by a contact force on the other hemisphere.

Let us define the set  $S$  of  $d + 1$  of the contacts on a given particle as a subset of the total contact network,  $S = \{\vec{r}_1, \vec{r}_2, \dots, \vec{r}_{d+1}\}$ . For this set  $S$ , we only need to check that any hemisphere that includes all of the contacts  $\vec{r}_2$  through  $\vec{r}_{d+1}$  does *not* also include  $\vec{r}_1$ , because then it is possible to attain a zero net force of zero. The boundaries of this set of dividing hemispheres that include  $\vec{r}_2$  through  $\vec{r}_{d+1}$  exactly coincide with the planes (or lines in 2D, hyperplanes in 4D, and so on) formed by every subset of  $d - 1$  of these vectors. These planes can be defined by their normal vectors, and can be computed by taking a  $d$ -dimensional generalization of the cross product of  $d - 1$  vectors, defined as the matrix determinant:

$$\text{cross}(\vec{v}_1, \vec{v}_2, \dots, \vec{v}_{d-1}) = \det \begin{bmatrix} v_{11} & v_{12} & \dots & v_{1d} \\ v_{21} & v_{22} & & \\ \vdots & & \ddots & \\ v_{(d-1)1} & & & v_{(d-1)d} \\ \hat{e}_1 & \hat{e}_2 & \dots & \hat{e}_d \end{bmatrix} \quad (1)$$

where  $v_{ij}$  is the  $j$ th component of vector  $i$  and  $\hat{e}_i$  is the  $i$ th unit basis vector. We define the cross product of  $d - 1$  of the vectors  $\vec{r}_2$  through  $\vec{r}_{d+1}$  as  $\vec{c}_i$ , where  $i$  is the index of the vector *not* included in the cross product. Then, putting all of this together, we find that  $\vec{r}_1$  is always on the opposite hemisphere of the particle from vectors  $\vec{r}_2$  through  $\vec{r}_{d+1}$  if and only if it is on the opposite side of  $\vec{r}_i$  with respect to the plane defined by  $\vec{c}_i$  for every  $i$  from 2 to  $d + 1$ . In other words, if you can find any set of  $d + 1$  contacts on a given particle for which

$$\frac{\vec{r}_1 \cdot \vec{c}_i}{\vec{r}_i \cdot \vec{c}_i} < 0 \quad (2)$$

holds for every  $i$  from 2 to  $d + 1$ , then it is not a rattler. Otherwise, it is. Note that this quotient must be nonzero for any set of contacts as long as none of them are collinear, coplanar, and so on.

- 
- [1] J. N. Roux, Phys. Rev. E **61**, 6802 (2000).  
[2] S. Torquato, A. Donev, and F. H. Stillinger, Int. J. Solids Struct. **40**, 7143 (2003).  
[3] S. Torquato and F. H. Stillinger, Rev. Mod. Phys. **82**, 2633 (2010).  
[4] A. Donev, R. Connelly, F. H. Stillinger, and S. Torquato, Phys. Rev. E **75**, 051304 (2007).  
[5] K. VanderWerf, W. Jin, M. D. Shattuck, and C. S. O'Hern, Phys. Rev. E **97**, 012909 (2018).